Journal of the Korean Ceramic Society (2021) 58:422–429
https://doi.org/10.1007/s43207-020-00107-z

ORIGINAL ARTICLE

Design, characterization and mechanical properties of new Na^+, CO_3^{2-}-apatite/alginate/C_{60} fullerene hybrid biocomposites

Nataliia Strutynska[1] · Anna Malyshenko[2] · Nina Tverdokhleb[3] · Maxim Evstigneev[3] · Ludmila Vovchenko[1] · Yuriy Prylutskyy[1] · Nikolai Slobodyanik[1] · Uwe Ritter[4]

Received: 22 September 2020 / Revised: 23 December 2020 / Accepted: 31 December 2020 / Published online: 26 January 2021

Abstract
Nanoparticles (20–50 nm) of Na^+, CO_3^{2-}-containing calcium phosphate (Na: 1.49 wt% and C: 1.53 wt%) with apatite-type structure were prepared by precipitation method from aqueous solution. According to FTIR spectroscopy data, the partial substitution of phosphate by carbonate (B-type) realized in the apatite-type structure. Obtained Na^+, CO_3^{2-}-hydroxyapatite (HAP) was used for the preparation of hybrid biocomposites with Alginate (Alg) with weight ratio HAP: Alg = 1:1 or 2:1 and C_{60} fullerene (C_{60}; from 0.2 to 4 wt%) and their mechanical properties were determined. It was found, that sample with weight ratio HAP: Alg = 2:1 and containing 4.0 wt% of C_{60} has the highest Young's modulus 429 MPa comparing with other determined samples. The structure modeling of the investigated system showed that the formation of triple complexes Na^+, CO_3^{2-}-HAP–Alg–C_{60} is stabilized by solvophobic and stacking interactions. The created biocomposites can be used as an effective implant material for bone restoration.

Keywords Chemical preparation · Composites · Mechanical properties · Apatite · Alginate

1 Introduction

The design of composites containing hydroxyapatite (HAP) with other materials represents one of the most promising strategies in developing effective biomaterials for bone regeneration. This approach is mainly based on the imitation of the composition and structure of human hard tissues, which are a real typical nanocomposites containing the polymer and ceramic components [1–13].

Ceramic component such as hydroxyapatite demonstrates adequate osteoconductivity and osteoinductivity as well as bright prospects in drug delivery field attributed to its characteristic pore structure, high surface area and chemical stability, but it has poor mechanical performance and uncontrollable biodegradability [2, 5, 10]. Taken into account, that most of the biological apatites contain several foreign ions, mainly carbonate (CO_3^{2-}) and traces of Na^+, Mg^{2+}, HPO_4^{2-}, F^- [14, 15], the synthetic HA are modified by different ions in order to influence on its properties. Thus, carbonate ions in apatite structure play a vital role in the bone and can influence the structure and morphology of the apatite [16, 17]. It should be noted, that carbonated apatite is bioceramic that has been shown to have high osteoconductivity and can be degraded. Thus, the use of carbonated apatite in bone tissue engineering applications is more appropriate than HAP because it is chemically more similar to bone apatite [18] and has a higher rate of resorption.

The natural and synthetic polymers such as collagen [19], alginate (Alg) [19–22], gelatin [23], poly(lactic acid), poly(glycolic acid) [24], chitosan [25–28], etc. can be used as components for hybrid biocomposites. Among all known polymers the sodium Alg is often used because of the low cost, biocompatibility [19, 22–24] and biodegradability [19, 22]. It can be made porous [22], non-toxic, and has the ability to modify the surface to generate the appropriate flexibility to suit its function. Previously it was shown that Alg

✉ Nataliia Strutynska
Strutynska_N@bigmir.net

1 Chemistry Department, Taras Shevchenko National University of Kyiv, 64/13, Volodymyrska Str., Kyiv 01601, Ukraine

2 Bogomolets National Medical University, Peremogy Ave. 34, Kyiv 03055, Ukraine

3 Sevastopol State University, Sevastopol 299053, Ukraine

4 Institute of Chemistry and Biotechnology, Technical University of Ilmenau, Weimarer Str., 25, 98693 Ilmenau, Germany

has been commonly used for drug delivery application [20, 22] and encapsulation [20, 21].

Thus, the combination of Alg as polymer component with chemically modified hydroxyapatite as a ceramic component allows to obtain hybrid biocomposite with optimum mechanical properties and tissue interaction. At the same time obtained scaffold must be biocompatible and has compatibility in living tissue, not cause foreign body response, and non-being toxic.

On the other hand, recent progress has increased interest in the biomedical application of the carbon nanostructure—C_{60} fullerene (C_{60}) that demonstrates unique physicochemical properties. Water-soluble pristine C_{60} is able to penetrate the cell membrane [29–31] and be non-toxic in vitro and in vivo systems [32] to exert specific health effects (e.g., antibacterial and antiviral) [33–35]. C_{60} is a spherical-like molecule, which surface consists of 60 carbon atoms, interconnected with single and double chemical bonds. The last is electron deficient, which determines the electron-acceptor properties of the molecule and its ability to attach reagents containing unpaired electrons (free radicals) easily [36–38]. Due to this ability, in biological systems C_{60} acts as a powerful scavenger of reactive oxygen species (ROS), allowing it to exhibit anti-inflammatory properties [39, 40]. C_{60} is a highly stable compound does not react with oxygen, is resistant to the action of alkalis and acids. Based on foregoing, C_{60} can be as an effective nanoplatform for the delivery of anticancer drugs [41, 42].

Thereby, the aim of this work focuses on the preparation of hybrid bioactive scaffolds based on apatite-related Na^+, CO_3^{2-}-containing calcium phosphate, Alginate and C_{60} fullerene for biomedical application. On the first step, the chemically modified calcium phosphate has been prepared and characterized. Then it was used for fabrication of hybrid biocomposites with different amount of Alg and C_{60}. The mechanical properties of the prepared biocomposites were investigated as well as structural modeling of Na^+, CO_3^{2-}-HAP–Alg–C_{60} system was done.

2 Experimental

2.1 *Synthesis of Na^+, CO_3^{2-}-containing apatite nanoparticles*

Apatite-related Na^+, CO_3^{2-}-containing calcium phosphate was synthesized using the chemical precipitation method. As initial reagents, an analytical graded $Ca(NO_3)_2{\cdot}4H_2O$, Na_2CO_3 and NaH_2PO_4 were used. Na_2CO_3 and NaH_2PO_4 solutions were added to a solution of $Ca(NO_3)_2{\cdot}4H_2O$ under stirring. Interaction was held at fixed molar ratios Ca/P = 1.67 and $CO_3^{2-}/PO_4^{3-} = 1.5$ at temperature 25 °C. The reaction mixture was stirred for 2 h and then resulting slurry was filtrated and washed up several times with water. The obtained precipitate was dried overnight at 100 °C. The prepared phosphate was characterized and then used for the preparation of composites.

2.2 *Preparation of pristine C_{60} aqueous colloid solution and Na^+, CO_3^{2-}-HAP–Alg–C_{60} biocomposites*

The pristine C_{60} aqueous colloid solution (C_{60}FAS) was prepared by C_{60} transfer from toluene to water using continuous ultrasound sonication as described by Ritter et al. [43]. The obtained C_{60}FAS was characterized by 0.15 mg/ml C_{60} concentration, 99% purity, stability and homogeneity; the average size of nanoparticles was 80 nm [44].

On the first stage, the Na^+, CO_3^{2-}-HAP–C_{60} composites were prepared by mixing of Na^+, CO_3^{2-}-HAP powder with C_{60}FAS and with further evaporation of water. Then, the obtained Na^+, CO_3^{2-}-HAP–C_{60} mixture and the necessary amount of sodium Alg powder was well grinding in an agate mortar. Then 10 ml of water was added. The obtained Na^+, CO_3^{2-}-HAP–Alg–C_{60}/H_2O mixture was added dropwise into 0.1 M $Ca(NO_3)_2$ solution. The obtained microspheres were washed with distilled water, filtered, dried at 80 °C and analyzed.

2.3 Characterization techniques

The phase and chemical composition of prepared calcium phosphate were determined using X-ray powder diffraction (XRD) and elemental analysis methods, respectively. The diffractogram was obtained using a Shimadzu XRD-6000 diffractometer with Cu–Kα radiation. The range of the diffraction angles (2θ) was from 5 to 90° with step 0.02. The elemental composition of calcium phosphate was defined by atomic absorption spectroscopy (Thermo Electron M-Series instrument) and CHN elemental analysis (Elementar-Analysensysteme GmbH, Donaustraβe 7, D-63452, Germany).

Fourier-transform infrared spectroscopy (FTIR) spectra of prepared Na^+, CO_3^{2-}-HAP and Na^+, CO_3^{2-}-HAP-Alg-C_{60} biocomposites were measured with PerkinElmer Spectrum BX spectrometer as KBr pellets in the range 400–4000 cm^{-1} at room temperature. The resolution of the spectrometer is 1 cm^{-1}.

The morphology and crystallite size of the prepared Na^+, CO_3^{2-}–HAP particles were investigated using a scanning electron microscope (SEM; FEI Quanta 400 ESEM instrument). The powder was previously coated with the Au/Pd.

For measuring the strength under the uniaxial compression, the powder of Na^+, CO_3^{2-}-HAP and its hybrid composites with different amount of Alg and C_{60} were prepared in the form of tablets with diameter 5 mm and thickness

1.7–2.0 mm by cold pressing of granulated powders in molds using the hydraulic press (at ~100 MPa). Mechanical properties of prepared samples under loading were investigated using the original automated equipment [45].

2.4 Structural modeling

The spatial structure of the elementary cell of apatite was reported in [46] and was taken by us from the American Mineralogist Crystal Structure Database in the form of AMC-file (code 0002297). Four 2 × 2 cells of Na^+, CO_3^{2-}-HAP crystal structure with substitution of 2 calcium atoms with Na^+ and 2 phosphorous groups with CO_3^{2-} was built using the VESTA program (version 3.4.4) [47].

The structure of C_{60} was taken from the Protein Data Bank32 (PDB codes Ids C_{60}) [48], built using HyperChem 8.0 software and energy minimized using Gaussian09W on DFT (B3LYP) level of theory with 6-31G* basis set.

The structure of sodium Alginate was built using HyperChem 8.0 software (the Sugar Builder module) by alternating hyaluronic (HYL) and mannuronic (MAN) units, linked by α-1,4 glycosidic bonds. The length of the oligosugar was set in a way to cover the perimeter of the interface between HAP and C_{60} and comprised 17 units: $(HYL–MAN)_8$-HYL. The hydrogen atoms of sugar carboxyls were substituted by sodium atoms.

The structure of the triple complex Na^+, CO_3^{2-}-HAP–Alg–C_{60} was built using HyperChem 8.0 software and energy minimized using the molecular mechanics method MM+.

3 Results and discussion

3.1 Synthesis and characterization of chemically modified apatite-related calcium phosphate

On the first step, the chemically modified apatite-related calcium phosphate as a ceramic component of composites was prepared using chemical precipitation method from an aqueous solution according to the scheme:

$$(10-x)Ca^{2+} + yNa^{+} + (6-z)PO_4^{3-} + zCO_3^{2-} + 2OH^{-} \rightarrow Ca_{10-x}Na_y(PO_4)_{6-z}(CO_3)_z(OH)_2.$$

Obtained solid was filtrated, dried at 100 °C and characterized. According to XRD and SEM data, the sample dried at 100 °C is poorly crystalline calcium phosphate with the size of particles in the range of 20–50 nm (Fig. 1a).

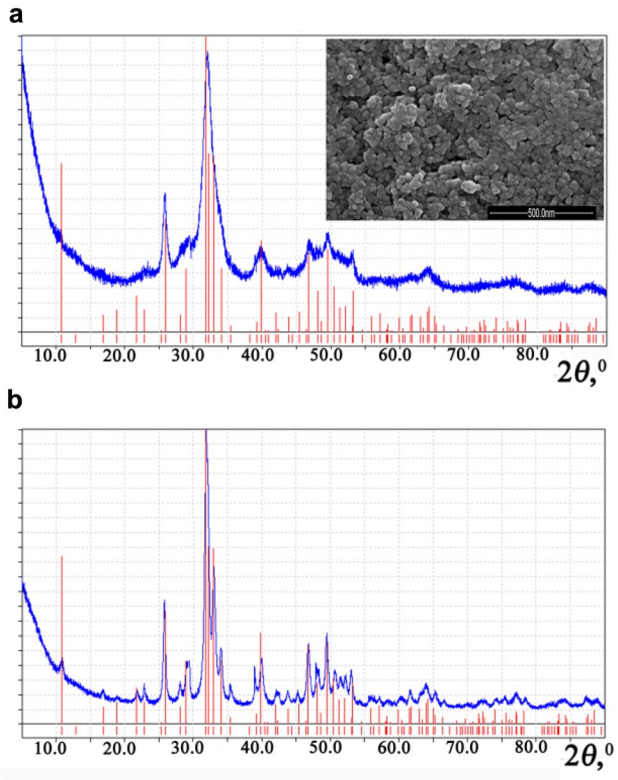

Fig. 1 XRD pattern and SEM image for prepared Na^+, CO_3^{2-}-containing calcium phosphate dried at 100 °C (**a**) and heated to 600 °C (**b**). $Ca_{10}(PO_4)_6O$ (ICDD, #01–089-6495, red color)

The chemical composition of prepared phosphate was determined using both an atomic absorption spectroscopy and CHN elemental analysis. The obtained results are the following: Ca: 26.47wt%, Na: 1.49 wt% and C: 1.53 wt%.

FTIR spectra for obtained powder showed the characteristic peaks of substituted calcium phosphate containing the carbonate anion. The adsorption bands at 879, 1440 and 1490 cm^{-1} correspond to the vibration of CO_3^{2-} and indicate the realization of B-type substitution of phosphate-group by carbonate in the apatite-type structure [49, 50]. Modes in the regions of 570–620 cm^{-1} and 980–1150 cm^{-1} were assigned to symmetric and asymmetric stretching vibrations (ν_4, ν_1 and ν_3) of phosphate tetrahedron, respectively. The broad peak in the range of (3275–3750) cm^{-1} appears due to sorbed water and the hydroxyl group stretching in apatite-type structure (Fig. 2, curve 1).

In order to confirm the formation of the apatite-related phase the obtained and dried at 100 °C sample was heated to 600 °C and characterized using the powder XRD method. The formation of apatite-related calcium phosphate that belongs to the hexagonal system was established. The calculated lattice parameters: $a = 9.409(6)$ and $c = 6.891(7)$ Å

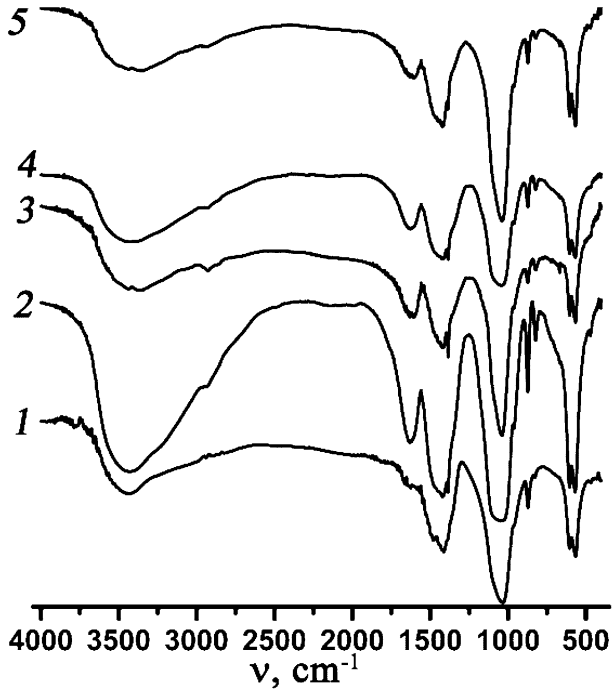

Fig. 2 FTIR spectra of the obtained samples: an initial Na^+, CO_3^{2-}-HAP (curve 1) and hybrid biocomposites: (Na^+, CO_3^{2-}–HAP: Alg) + C_{60} = (1: 1) + 0.2 wt% (curve 2); (2: 1) + 0.2 wt% (curve 3); (2: 1) + 2.0 wt% (curve 4); (2: 1) + 4.0 wt% (curve 5)

are close to corresponding values early reported in [49]. The formation of impurities was not detected (Fig. 1b).

Based on the XRD, SEM, FTIR and elemental analysis data the nanoparticles of apatite-type Na^+, CO_3^{2-}–calcium phosphate were prepared.

3.2 *Preparation and characterization of Na^+, CO_3^{2-}-HAP–Alg–C_{60} hybrid biocomposites*

Obtained chemically modified calcium phosphate was used as an inorganic component for the preparation of hybrid biocomposites with Alg and C_{60}. Four samples with different content of Alg and C_{60} were fabricated (Table 1). Photos of obtained biocomposite microspheres are shown in Fig. 3.

Table 1 Symbols for prepared biocomposites depending on their composition

Sample index	Weight ratio (Na^+, CO_3^{2-}-HAP: Alg)	Wt% C_{60}
N1	1:1	0.2
N2	2:1	0.2
N3		2.0
N4		4.0

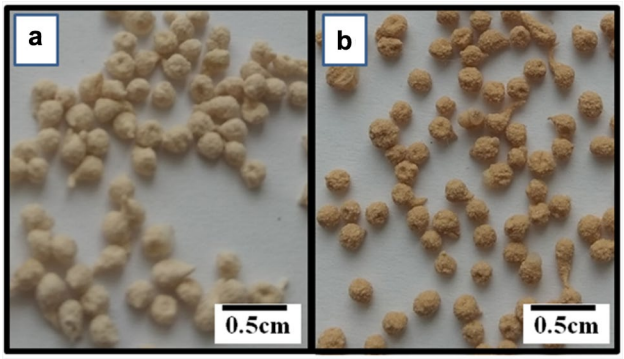

Fig. 3 Photos of dried at 80 °C microspheres of hybrid biocomposites (Na^+, CO_3^{2-}–HAP: Alg) + C_{60}= (2: 1) + 0.2 wt% (**a**) and (2: 1) + 2.0 wt% (**b**)

FTIR spectra of obtained Na^+, CO_3^{2-}-HAP–Alg–C_{60} biocomposites showed the characteristic vibrational bands of phosphate group PO_4 in apatite in the ranges 1190–960 cm^{-1} (ν_3) and 610–550 cm^{-1} (ν_4) (Fig. 2, curves 2–5). The main difference of the spectra of initial Na^+, CO_3^{2-}-HAP and obtained composites Na^+, CO_3^{2-}-HAP–Alg–C_{60} is the presence of mode at 1420 cm^{-1} that is assigned to the symmetric stretching vibration of the COO^- groups of Alg. The peak at 1630 cm^{-1} corresponding to the asymmetric stretching vibration of carbonyl (C = O) of Alg and intensivity of this band correlate with the amount of Alginate in composites (Fig. 2, curves 2–5). Besides, the evidence of methylene (CH_2) at 2850 cm^{-1} and 2920 cm^{-1} from the Alginate can be also observed in the spectra, which confirmed the existence of Alginate [51]. According to reported data, the characteristic FTIR vibrational modes for C_{60} are at 524, 574, 1182 and 1420 cm^{-1} [52]. In the spectra of prepared Na^+, CO_3^{2-}-HAP–Alg–C_{60} biocomposites, the peaks of C_{60} (at 524, 574, 1182 and 1420 cm^{-1}) overlap with vibrational bands of phosphate group PO_4 in apatite and vibration of Alginate.

3.3 Compressive strength of prepared samples

Results of the studies of compressive strength (σ_c) of initial apatite-related Na^+, CO_3^{2-}-containing calcium phosphate and prepared Na^+, CO_3^{2-}-HAP–Alg–C_{60} biocomposites are represented in Table 2 and Figs. 4, 5.

As it is seen from Fig. 4, only sample N1 (with weight ratio HAP: Alg = 1:1 and 0.2 wt% C_{60}) was destructed at relatively low compressive loading (~ 58 MPa) and maximal relative deformation ε_{destr} is equal to 0.22. Another three samples, namely N2, N3 and N4 (with weight ratio HAP: Alg = 2:1 and different amount of C_{60} (Table 1)) are flattened, its thickness was decreased on 30–60% (large relative deformation ε_{destr} = 0.36–0.63), while the diameter was increased. After unloading these samples are not restored, i.e. under

Table 2 Strength properties of initial apatite-related Na^+, CO_3^{2-}-containing calcium phosphate, prepared Na^+, CO_3^{2-}-HAP–Alg–C_{60} biocomposites (N1–N4) and literature data

Sample index	Density, g/cm^3	Max. relative deformation, ε_{destr}	Strength σ_c, MPa	Young's modulus E, MPa
Na^+, CO_3^{2-}-HAP	1.92	0.033	29	745
N1	1.58	0.22 (at 58 MPa)	58	343
N2	1.61	0.39 (at 121 MPa)	Sample is flattened at loading up to 121 MPa	394
N3	1.60	0.63 (at 241 MPa)	Sample is flattened at loading up to 241 MPa	327
N4	1.69	0.36 (at 184 MPa)	Sample is flattened at loading up to 184 MPa	429
Hydroxyapatite [53]	–	≈ 1.0	40	≈400
HAP/Alginate composite [54]	1.46	–	47	–
HAP/poly(sorbitol sebacate malate) composite [55]	–	–	23	627

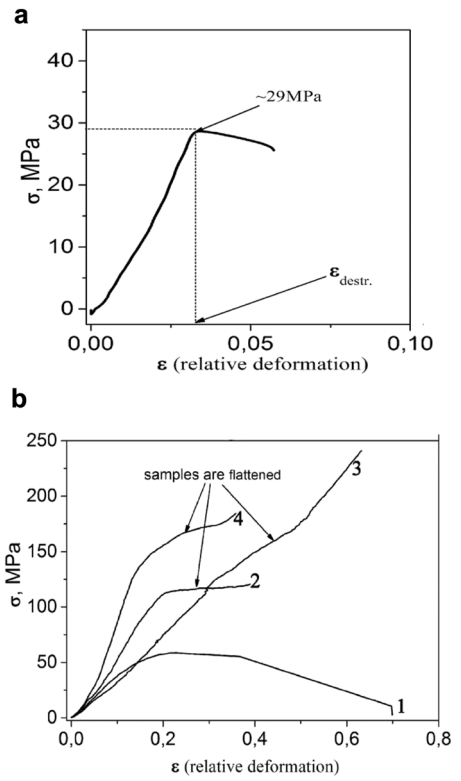

Fig. 4 Strength σ_c of obtained samples: an initial Na^+, CO_3^{2-}-HAP (**a**) and hybrid biocomposites: ((Na^+, CO_3^{2-}-HAP: Alg)+C_{60})=(1: 1)+0.2 wt% (curve 1); (2: 1)+0.2 wt% (curve 2); (2: 1)+2.0 wt% (curve 3); (2: 1)+4.0 wt% (curve 4) measured at uniaxial compression

compression up to loading in 121–241 MPa the large plastic deformations occur, that may lead to ductile failure. Figure 5 presents the "loading–unloading" diagrams $\sigma(\varepsilon)$ of investigated samples during three cycles of uniaxial compression up to 12 MPa. The Young's modulus (E) estimation has shown that maximal value of E=429 MPa was observed for the sample N4 (with weight ratio HAP: Alg=2:1 and 4.0 wt% C_{60}), and for other samples, N1, N2 and N3, the value of E lies within (327–394) MPa. This result indicates the influence of C_{60} addition to Phosphate-Alginate mixture on the mechanical properties of hybrid composites.

Summarizing, prepared biocomposites in system Na^+, CO_3^{2-}-HAP–Alg–C_{60} can be used as biomaterials with special mechanical properties for bone restoration as well as in delivery systems with controlled drug release [56].

3.4 *Structural modeling of Na^+, CO_3^{2-}–HAP–Alg–C_{60} system*

The possibility of complexation between the components of designed hybrid biocomposite was testified by means of molecular mechanics. The model of 3D structure of the triple Na^+, CO_3^{2-}-HAP–Alg–C_{60} complex is shown on Fig. 6. Such arrangement of molecules is mainly stabilized by solvophobic/van der Waals interactions between the C_{60} and Na^+, CO_3^{2-}-HAP surfaces, and is additionally stabilized by the hydrogen bonds between the OH-groups of Alg and oxygen atoms of Na^+, CO_3^{2-}-HAP (≈2 bonds).

Within the framework of the MM+ method, we calculated the energies of intra- and intermolecular interactions in the triple complex, viz.

$E_{\text{total}} = 3142.54$ kcal/mol, $E_{C_{60}} = 224.63$ kcal/mol, $E_{Na^+,CO_3^{2-}\text{-HAP}} = 1259.86$ kcal/mol, $E_{\text{Alg}} = 1672.92$ kcal/mol.

It allowed to estimate the contribution of the intermolecular interactions into the total energy of complex formation: $\Delta E = E_{\text{total}} - E_{C_{60}} - E_{Na^+,CO_3^{2-}\text{-HAP}} - E_{\text{Alg}} \approx -14.88$ kcal/mol. This value should be increased by the magnitude of complex stabilization from solvophobic interactions. The latter could be estimated from solvent accessible surface areas, A, of each molecule in separate and in complex, viz. $A_{\text{total}} = 5373.72$ Å^2, $A_{C_{60}} = 524.82$ Å^2, $A_{Na^+,CO_3^{2-}\text{-HAP}} = 2597.03$ Å^2, $A_{\text{Alg}} = 3775.57$ Å^2. Taking the microscopic surface tension,

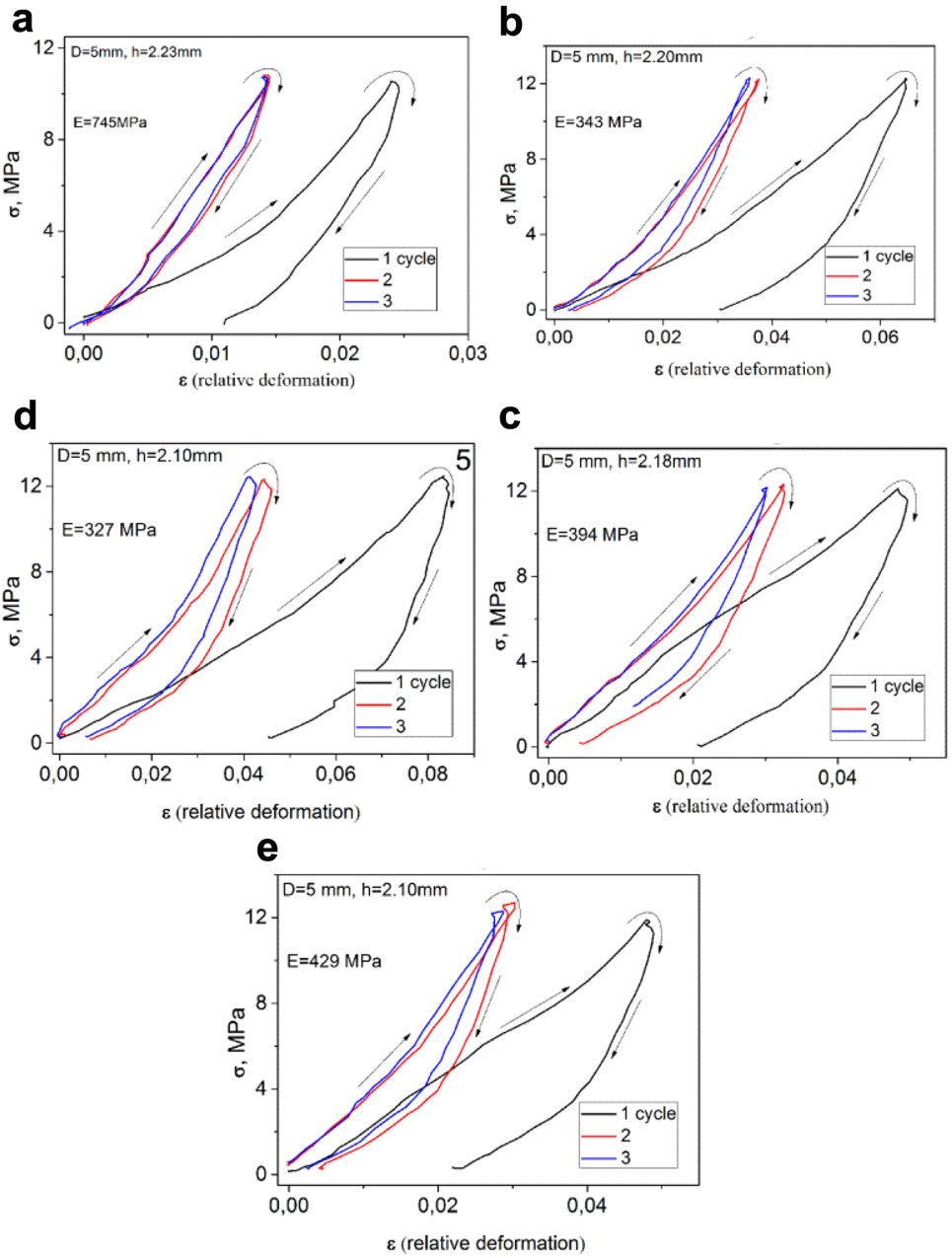

Fig. 5 "Loading–unloading" diagrams $\sigma(\varepsilon)$ of obtained samples: an initial Na^+, CO_3^{2-}-HAP (**a**) and hybrid biocomposites: (Na^+, CO_3^{2-}-HAP: Alg) + C_{60} = (1: 1) + 0.2 wt% (**b**); (2: 1) + 0.2 wt% (**c**); (2: 1) + 2.0 wt% (**d**); (2: 1) + 4.0 wt% (**e**) measured at uniaxial compression during three loading cycles

$\gamma = 0.05$ kcal/mol·Å^2, for water [57], one can finally estimate the solvophobic contribution as $\Delta G_{hyd} = \gamma(A_{total} - A_{C_{60}} - A_{Na^+,CO_3^{2-}}\text{-HAP} - A_{Alg}) \approx -76.19$ kcal/mol. It is seen that the energy of solvophobic interactions in absolute value is more than the absolute value of total stabilization energy. It means that some contributions can be positive and destabilize complex, whereas contributions from van der Waals stacking energy and H-bonds are small in absolute value.

In summary, it may be concluded that the physical adsorption of C_{60} into Na^+, CO_3^{2-}-HAP–Alg system seems possible by means of forming triple complexes stabilized by solvophobic and stacking interactions, whereas H-bonds give relatively small contribution into stabilization.

4 Conclusion

According to the powder XRD, SEM, FTIR and elemental analysis data the nanoparticles (20–50 nm) of apatite-related Na^+, CO_3^{2-}-containing calcium phosphate were prepared. Then, obtained inorganic component was used for the design of hybrid biocomposites Na^+, CO_3^{2-}-HAP–Alg–C_{60} with different amounts of Alg and C_{60}. Studies of compressive strength of prepared Na^+, CO_3^{2-}-HAP–Alg–C_{60} biocomposites showed that sample containing 4.0 wt% of C_{60} (with weight ratio HAP: Alg = 2:1) has the highest Young's modulus 429 MPa. This result may be indicated that the addition of C_{60} into apatite-Alg composite influence on its

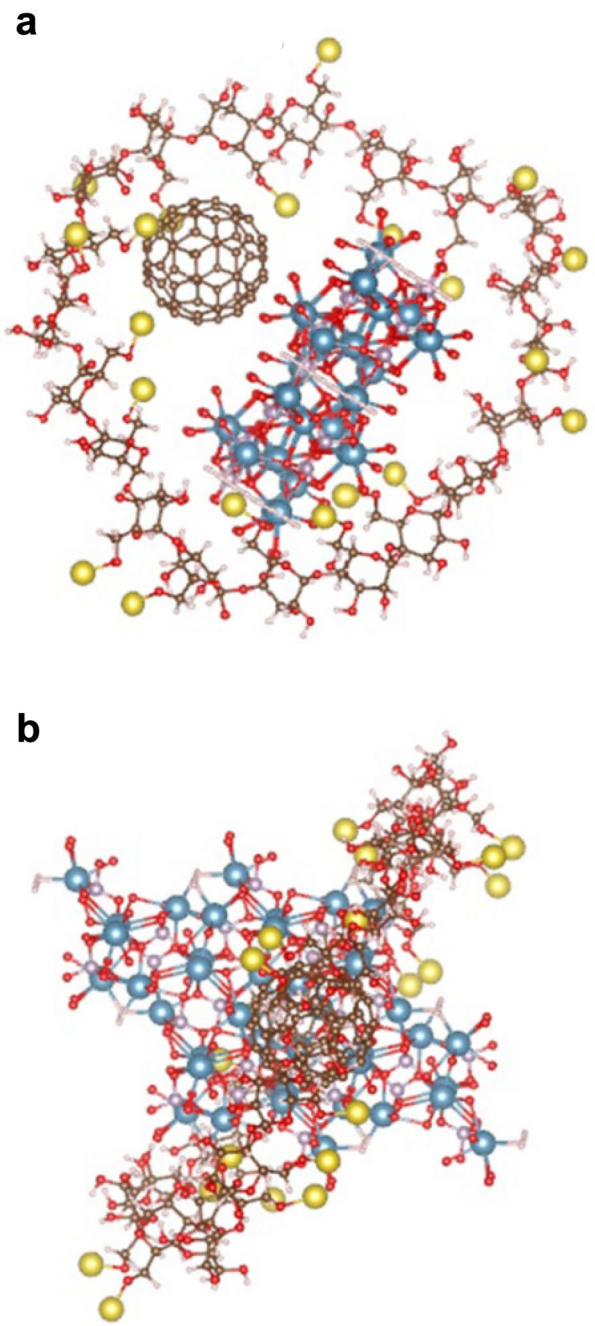

Fig. 6 The calculated spatial structures of Na^+, CO_3^{2-}-HAP–Alg–C_{60} triple complex: top view (**a**) and side view (**b**)

mechanical properties. Results of structural modeling of Na^+, CO_3^{2-}-HAP–Alg–C_{60} system showed that the physical adsorption of C_{60} into Na^+, CO_3^{2-}-HAP–Alg composite seems possible by means of forming triple complexes stabilized by solvophobic and stacking interactions.

Hereby, the subject and results of the presented investigation have by both methodological meaning as the general approach to study interaction inorganic particles with organic substance and can be used for practical fabrication of effective materials in system Na^+, CO_3^{2-}-HAP–Alg–C_{60} with special mechanical properties for biomedical applications.

Acknowledgements This work was partially supported by the DFG (N RI 966/18-1).

References

1. R. Zhang, P.X. Ma, J Biomed Mater Res **44**, 446 (1999)
2. S.J. Peter, L. Lu, D.J. Kim, A.G. Mikos, Biomaterials **21**, 1207 (2000)
3. G. Wei, P.X. Ma, Biomaterials **25**, 4749 (2004)
4. S.S. Kim, M.S. Park, S.J. Gwak, C.Y. Choi, B.S. Kim, Tissue Eng **12**, 2997 (2006)
5. S.S. Kim, M.S. Park, O. Jeon, C.Y. Choi, B.S. Kim, Biomaterials **27**, 1399 (2006)
6. K.M. Woo, J. Seo, R. Zhang, P.X. Ma, Biomaterials **28**, 2622 (2007)
7. X.L. Deng, G. Sui, M.L. Zhao, G.Q. Chen, X.P. Yang, J Biomater Sci **8**, 117 (2007)
8. S.W. Kang, H.S. Yang, S.W. Seo, D.K. Han, B.S. Kim, J Biomed Mater Res A **85**, 747 (2008)
9. J. Li, X. Yuan, F. He, A.F. Mak, J Biomed Mater Res **86B**, 381 (2008)
10. K.H. Włodarski, P.K. Włodarski, R. Galus, Ortop Traumatol Rehabil **10**(3), 201 (2008)
11. P. Zhang, Z. Hong, T. Yu, X. Chen, X. Jing, Biomaterials **30**, 58 (2009)
12. J. Venkatesan, I. Bhatnagar, P. Manivasagan, K.-H. Kang, S.-K. Kim, J Biolog Macromol **72**, 269 (2015)
13. K. Jahan, M. Tabrizian, Biomater Sci **4**(1), 25 (2016)
14. R.Z. LeGeros, Nature **206**, 403 (1965)
15. A. Bigi, G. Cojazzi, S. Panzavolta, A. Ripamonti, N. Roveri, M. Romello, J Inorg Biochem **68**, 45 (1997)
16. G. Xu, I.A. Aksay, J.T. Groves, J Am Chem Soc **123**, 2196 (2001)
17. A. Krajewski, M. Mazzocchi, P.L. Buldini, A. Ravaglioli, A. Tinti, P. Taddei, C. Fagnano, J Mol Struct **744–747**, 221 (2005)
18. I.D. Ana, S. Matsuya, K. Ishikawa, Engineering **2**, 344 (2010)
19. G.H. Kim, S.H. Ahn, Y.Y. Kim, Y.S. Cho, W. Chun, J Mater Chem **21**, 6165 (2011)
20. C.K. Kuo, P.X. Ma, Biomaterials **22**, 511 (2001)
21. N. Mohan, P.D. Nair, Trends Biomater Artif Org **18**(2), 219 (2005)
22. J.-W. Lu, Y.-L. Zhu, Z.-X. Guo, P. Hu, J. Yu, Polymer **47**, 8026 (2006)
23. H.-W. Kim, B.-H. Yoon, H.-E. Kim, J Mater Sci **16**, 1105 (2005)
24. T.-J. Lee, S.-W. Kang, S.H. Bhang, J.M. Kang, B.-S. Kim, J Biomater Sci **21**, 635 (2010)
25. K. Tuzlakoglu, R.L. Reis, J Mater Sci Mater Med **18**, 1279 (2007)
26. C.I. Dias, J.F. Mano, N.M. Alves, J Mater Chem **18**, 2493 (2008)
27. A.R. Costa-Pinto, V.M. Correlo, P.C. Sol, M. Bhattacharya, P. Charbord, B. Delorme, R.L. Reis, N.M. Neves, Biomacromol **10**, 2067 (2009)
28. B. Li, Y. Wang, D. Jia, Y. Zhou, W. Cai, Biomed Mater **4**, 015011 (2009)
29. S. Foley, C. Crowley, M. Smaihi, C. Bonfils, B.F. Erlanger, P. Seta, C. Larroque, Biochem Biophys Res Commun **294**, 116 (2002)
30. C. Schuetze, U. Ritter, P. Scharff, A. Bychko, S. Prylutska, V. Rybalchenko, Yu. Prylutskyy, Mater Sci Eng C **31**, 1148 (2011)
31. Yu. Prylutskyy, A. Bychko, V. Sokolova, S. Prylutska, M. Evstigneev, V. Rybalchenko, M. Epple, P. Scharff, Mater Sci Eng C **59**, 398 (2016)

32. S.V. Prylutska, A.G. Grebinyk, O.V. Lynchak, I.V. Byelinska, V.V. Cherepanov, E. Tauscher, O.P. Matyshevska, Yu.I. Prylutskyy, V.K. Rybalchenko, U. Ritter, M. Frohme, Fuller Nanotubes Carbon Nanostruct **27**, 715 (2019)
33. C. Kepley, J Nanomed Nanotechnol **3**, 6 (2012)
34. S. Goodarzi, T. Da Ros, J. Conde, F. Sefat, M. Mozafari, Mater Today **20**(8), 460 (2017)
35. F. Moussa, Nanobiomaterials **25**, 113 (2018)
36. N. Gharbi, M. Pressac, M. Hadchouel, H. Szwarc, S.R. Wilson, F. Moussa, Nano Lett **5**(12), 2578 (2005)
37. C.A. Ferreira, D. Ni, Z.T. Rosenkrans, W. Cai, Nano Res **11**(10), 4955 (2018)
38. S.V. Eswaran, Curr Sci **114**(9), 1846 (2018)
39. V. Dragojevic-Simic, V. Jacevic, S. Dobric, A. Djordjevic, D. Bokonjic, M. Bajcetic, R. Injac, Dig J Nanomater Biostruct **6**, 819 (2011)
40. O.O. Gonchar, A.V. Maznychenko, N.V. Bulgakova, I.V. Vereshchaka, T. Tomiak, U. Ritter, Yu.I. Prylutskyy, I.M. Mankovska, A.I. Kostyukov, Oxidative Med Cell Longev **2018**, 17 (2018)
41. Yu.I. Prylutskyy, M.P. Evstigneev, V.V. Cherepanov, O.A. Kyzyma, L.A. Bulavin, N.A. Davidenko, P. Scharff, J Nanopart Res **17**, 45 (2015)
42. S. Prylutska, R. Panchuk, G. Gołuński, L. Skivka, Yu. Prylutskyy, V. Hurmach, N. Skorokhyd, A. Borowik, A. Woziwodzka, J. Piosik, O. Kyzyma, V. Garamus, L. Bulavin, M. Evstigneev, A. Buchelnikov, R. Stoika, W. Berger, U. Ritter, P. Scharff, Nano Res **10**(2), 652 (2017)
43. U. Ritter, Y.I. Prylutskyy, M.P. Evstigneev, N.A. Davidenko, V.V. Cherepanov, A.I. Senenko, O.A. Marchenko, A.G. Naumovets, Fuller Nanotub Carbon Nanostruct **23**, 530 (2015)
44. Yu.I. Prylutskyy, V.V. Cherepanov, M.P. Evstigneev, O.A. Kyzyma, V.I. Petrenko, V.I. Styopkin, L.A. Bulavin, N.A. Davidenko, D. Wyrzykowski, A. Woziwodzka, J. Piosik, R. Kaźmierkiewicz, U. Ritter, Phys Chem Chem Phys **17**, 26084 (2015)
45. L. Vovchenko, O. Lazarenko, L. Matzui, Yu. Perets, A. Zhuravkov, V. Fedorets, F. Le Normand, Phys Status Solid A **211**, 336 (2014)
46. R.M. Wilson, J.C. Elliot, S.E.P. Dowker, Am Miner **84**, 1406 (1999)
47. K. Momma, F. Izumi, J Appl Crystallogr **44**, 1272 (2011)
48. H.M. Berman, J. Westbrook, Z. Feng, G. Gilliland, T.N. Bhat, H. Weissig, I.N. Shindyalov, P.E. Bourne, Nucleic Acids Res **28**, 235 (2000)
49. N. Strutynska, I. Zatovsky, N. Slobodyanik, A. Malyshenko, Y. Prylutskyy, O. Prymak, I. Vorona, S. Ishchenko, N. Baran, A. Byeda, A. Mischanchuk, Eur J Inorg Chem **2015**, 622 (2015)
50. N. Strutynska, N. Slobodyanik, A. Malyshenko, I. Zatovsky, I. Vorona, Y. Prylutskyy, O. Prymak, N. Baran, S. Ishchenko, V. Nosenko, Solid State Phenom **230**, 133 (2015)
51. L.B. Sukhodub, L.F. Sukhodub, O.O. Litsis, Yu.I. Prylutskyy, Mater Chem Phys **217**, 228 (2018)
52. Yu.I. Prylutskyy, V.I. Petrenko, O.I. Ivankov, O.A. Kyzyma, L.A. Bulavin, O.O. Litsis, M.P. Evstigneev, V.V. Cherepanov, A.G. Naumovets, U. Ritter, Langmuir **14**, 3967 (2014)
53. R.Z. LeGeros, J.P. LeGeros, in *An introduction to bioceramics*. ed. by L.L. Hench, J. Wilson (Word Scientific, London, 1999), p. 139
54. N. Kanasan, S. Adzila, N.A. Mustaffa, P. Gurubaran, Proc Eng **184**, 442 (2017)
55. W.H. Tham, M.U. Wahit, M. Rafiq, A. Kadir, T.W. Wong, Songklanakarin. J Sci Technol **35**(1), 57–61 (2013)
56. L.B. Sukhodub, L.F. Sukhodub, M.O. Kumeda, S.V. Prylutska, V. Deineka, Yu.I. Prylutskyy, U. Ritter, Carbohydr Polym **223**, 115067 (2019)
57. V.V. Kostjukov, N.M. Khomytova, A.A.H. Santiago, A.M.C. Tavera, J.S. Alvarado, M.P. Evstigneev, J Chem Thermodyn **43**(10), 1424 (2011)